Article

Discovery Medicine 2025; 37(193): 286–298
https://doi.org/10.24976/Discov.Med.202537193.23

Urolithin B Promotes Meniscal Regeneration and Prevents the Development of Osteoarthritis in Mice

Wenjun Wang[1], Husheng Wang[2], Lin Wang[2], Yalin Zhang[2], Huihui Liu[3], Binbin Ci[2,*]

[1]Department of Emergency, Wendeng Hospital of Traditional Chinese Orthopedics and Traumatology of Shandong Province, 264400 Weihai, Shandong, China
[2]Department of Orthopedics, Wendeng Hospital of Traditional Chinese Orthopedics and Traumatology of Shandong Province, 264400 Weihai, Shandong, China
[3]Department of Pharmacy, Wendeng Hospital of Traditional Chinese Orthopedics and Traumatology of Shandong Province, 264400 Weihai, Shandong, China
*Correspondence: cibinbin2023@sina.com (Binbin Ci)
Published: 20 February 2025

Background: Osteoarthritis (OA) is one of the most prevalent arthritis types globally, with the knee being particularly susceptible due to its frequent and strenuous use. Urolithin B (UB) exhibits various biological properties, with meniscal repair playing an important role in preventing knee OA. This study aimed to explore the impact of UB on meniscal regeneration and OA progression.

Methods: Initially, we explored the effect of UB on meniscal cells. Utilizing the cell counting kit (CCK)-8 assay, we determined the optimum concentration of UB treatment. Enzyme-linked immunosorbent assay (ELISA) was used for detecting inflammation-related interleukin-1beta (IL-1β). Real-time reverse transcriptase-polymerase chain reaction (RT-qPCR) was used for measuring the expression of extracellular matrix (ECM)-related proteins, ECM-degrading enzymes, and genes associated with joint formation in meniscal cells. Furthermore, 5-Bromo-2′-deoxyuridine (BrdU) staining was used to evaluate the proliferation of meniscal cells. Meniscal tissues were cultured *in vitro*, and western blot analysis was used to detect levels of proliferation-related markers such as proliferating cell nuclear antigen (PCNA) and vascular endothelial growth factor (VEGF), as well as ECM protein collagen-1 (COL-1) and ECM degradation-related matrix metallopeptidase-13 (MMP-13). Mice were subjected to meniscus injury to establish a knee joint model of meniscus injury-induced osteoarthritis (MIOA) and to verify the effect of UB on meniscal cells *in vivo*. Pathological changes in knee joints were observed using hematoxylin-eosin (H&E) staining. Additionally, western blot was used to assess PCNA, VEGF, COL-1, and MMP-13 levels, while ELISA was used to detect inflammation-related tumor necrosis factor-alpha (TNF-α), IL-1β, IL-6, and interferon-gamma (IFN-γ) in mouse menisci.

Results: At concentrations up to 100 µM, UB exhibited non-toxicity and concomitantly decreased IL-1β in meniscal cells ($p < 0.001$). Moreover, UB increased the expression of ECM-related proteins ($p < 0.001$) and genes associated with joint formation ($p < 0.001$), while concurrently decreasing the expression of ECM-degrading enzymes ($p < 0.001$) in meniscal cells. UB promoted meniscal cell proliferation ($p < 0.001$). Additionally, UB increased PCNA, VEGF, and COL-1 while suppressing MMP-13 in menisci cultured *in vitro* ($p < 0.001$). Moreover, UB mitigated the pathological alterations observed in knee joints affected by meniscus injury. In murine models, MIOA led to decreased PCNA, VEGF, and COL-1 levels, alongside increased MMP-13, TNF-α, IL-1β, IL-6, and IFN-γ levels ($p < 0.001$), all of which were effectively reversed by UB treatment ($p < 0.001$).

Conclusion: UB effectively promotes meniscal regeneration and repair, while protecting against knee OA in mice, suggesting its potential role in clinical OA treatment.

Keywords: osteoarthritis; urolithin B; knee osteoarthritis; meniscal regeneration; extracellular matrix

Introduction

Osteoarthritis (OA) is one of the most common arthritis types, characterized by chronic degenerative changes within the entire synovial joint, potentially leading to disability [1]. Among all joints potentially affected by OA, the knee is most commonly affected by OA due to its frequent and strenuous use [2]. Knee and hip OA have collectively become the leading cause of global disability [3]. However, non-surgical OA treatments remain limited for knee OA despite the increased OA rate, often necessitating knee joint replacement [4]. Clinical OA treatments often focus on mitigating joint pain rather than suppressing OA progression [5]. As a result, there is a pressing need for deeper insights into OA pathogenesis to develop non-surgical interventions that effectively slow its progression and provide supplementary guidance for treatment strategies.

Knee OA is generally associated with multiple tissues including the menisci [6]. The meniscus is a crescent-shaped fibrocartilage located between the tibial plateau and the femoral condyle, playing essential roles in shock absorption, lubrication, and stabilization of the knee joint [7]. Given that meniscal injury often reduces meniscal function and commonly precedes OA development, repair is highly recommended whenever possible [6,8]. Accordingly, native meniscus tissue regeneration is preferred over meniscal resection, not only for treating but also for preventing and restoring injured meniscal tissues [8].

Urolithin B (UB) is a natural compound produced by gut bacteria and is recognized as one of the major metabolites of ellagic acid [9,10]. Previous studies have demonstrated UB's diverse biological activities, including neuroprotection, cardiovascular protection, renal protection, anticancer properties, anti-inflammatory effects, antioxidant properties, antidiabetic effects, and antibacterial properties [11–13]. Notably, urolithin A (UA), another major metabolite of ellagic acid, has been shown to alleviate OA by improving mitochondrial health [14]. However, drugs targeting OA are lacking and alternatives for alleviating OA are still needed. We hypothesized and explored the potential impact of UB on OA.

In the present study, we performed studies both *in vitro* and *in vivo* to explore the effect of UB on meniscal tissue. Given the pivotal role of meniscal repair and regeneration in OA prevention, we also examined UB's effects on OA progression. The findings in this study aim to enhance the novel understanding of UB's role in OA pathogenesis and offer UB as a potential therapeutic agent for OA treatment and prevention by promoting meniscal repair.

Materials and Methods

Meniscal Cell Culture and Treatment

Mouse meniscal cells were purchased (MIC-iCell-s039, iCell Bioscience Inc., Shanghai, China) and cultured in a system specifically designed for primary chondrocytes (PriMed-iCell-020, iCell bioscience Inc., Shanghai, China) under 37 °C and 5% CO_2. The cells were authenticated by mycoplasma testing, which was performed to ensure the absence of contamination. The cells were observed with a high power microscope (BX53M, Olympus, Tokyo, Japan). Mouse interleukin-1beta (IL-1β) protein was purchased (HY-P700187AF, MedChemExpress, Monmouth Junction, NJ, USA) and added into the culture system (1 ng/mL for 12 h [15]) to increase basal tumor necrosis factor-alpha (TNF-α) protein levels. Urolithin B (HY-126307, MedChemExpress, Monmouth Junction, NJ, USA) was added to the culture system according to the treatment protocols.

Immunofluorescence

The cells were fixed with 4% paraformaldehyde for 15 minutes. Inject 0.1% Triton X-100 into PBS for 10 minutes. After that, the cells were sealed with 2% BSA for 15 minutes. Incubate COL-1 (ab138492, Abcam, Cambridge, MA, USA) or COL-2 (ab34712, Abcam, Cambridge, MA, USA) overnight at 4°C. The next day, the secondary antibody (ab150079, Abcam, Cambridge, MA, USA) was washed with PBS 3 times and incubated at room temperature for 2 hours. After washing with PBS for three times, dye with DAPI (C0065, Solarbio, Beijing, China) for 10 minutes. Finally, the images were observed with a microscope (CX41-32RFL, Olympus, Tokyo, Japan).

Cell Counting Kit (CCK)-8 Assay

Cells subjected to various treatments were seeded in 96-well culture plates at a density of 1×10^4 cells/well and incubated for either two days or five days at 37 °C with 5% CO_2. Subsequently, the medium was discarded and replaced with 95 µL of normal medium and supplemented with 5 µL of cell counting kit (CCK)-8 reagent (C0037, Beyotime, Shanghai, China). After incubation for 2 h, the microplate reader (CMax Plux, Molecular Devices, Shanghai, China) was used to measure the optical density (OD) value at 450 nm to assess cell viability.

Cell viability (%) = [(As – Ab) / (Ac – Ab)] × 100%

As: experimental hole absorbance; Ac: control hole absorbance; Ab: blank hole absorbance.

Enzyme-Linked Immunosorbent Assay (ELISA)

Following the manufacturer's instructions, enzyme-linked immunosorbent assay (ELISA) kits were used to evaluate the levels of IL-1β (EK201B, MultiSciences, Hangzhou, China), TNF-α (ab100747, Abcam, Cambridge, MA, USA), interleukin-6 (IL-6; ab222503, Abcam, Cambridge, MA, USA), and interferon-gamma (IFN-γ; ab282874, Abcam, Cambridge, MA, USA). The concentrations were presented in pg/mL.

The Real-Time Reverse Transcriptase-Polymerase Chain Reaction (RT-qPCR)

The total RNA was extracted from cells using the TRIzol reagent (R0016, Beyotime, Shanghai, China) and reversely transcribed into cDNA using FastQuant cDNA (KR116, Tiangen, Beijing, China). The cDNA was amplified using a PCR instrument (LightCycler96, Roche, Shanghai, China) with the following program: predenaturation at 95 °C for 10 s, annealing at 60 °C for 30 s, and extension for 40 s over 40 cycles. β-*actin* served as an internal reference and relative mRNA levels were calculated using the $2^{-\Delta\Delta Ct}$ method. Table 1 lists the primer sequences.

Animal Preparation

Thirty male C57BL/6J WT mice (25–30 g) aged three months were purchased from Jinan Pengyue Laboratory Animal Technology Co., Ltd. (Jinan, China) and housed with free access to food and water under controlled condi-

Table 1. Primer sequences.

Name	Primer sequences (5′-3′)
Col-1	F GCTCCTCTTAGGGGCCACT
	R ATTGGGGACCCTTAGGCCAT
Col-2	F GGGTCACAGAGGTTACCCAG
	R ACCAGGGGAACCACTCTCAC
Col-3	F ACGTAAGCACTGGTGGACAG
	R GGAGGGCCATAGCTGAACTG
Aggrecan	F AAGTGCTATGCTGGCTGGTT
	R GGTCTGGTTGGGGTAGAGGT
Mmp-13	F CCAGAACTTCCCAACCAT
	R ACCCTCCATAATGTCATACC
Adamts4	F CCTGGCAAGGACTATGATGCTGA
	R GGGCGAGTGTTTGGTCTGG
Adamts5	F GCAGAACATCGACCAACTCTACTC
	R CCAGCAATGCCCACCGAAC
Timp-1	F CCCTTTGCATCTCTGGCATC
	R GCATTTCCCACAGCCTTGAA
Sox6	F GAGCCCAGGTTTGTCTCCATC
	R CCAGCGAGGAAGAGAAATTGC
Sox9	F AGTACCCGCATCTGCACAAC
	R ACGAAGGGTCTCTTCTCGCT
Runx2	F TTCAACGATCTGAGATTTGTGGG
	R GGATGAGGAATGCGCCCTA
Ki67	F GCCTCCTAATACACCACTGAA
	R GCCGTTCCTTGATGATTGTC
Gdf5	F CCATCACACCCCACGAATACA
	R GCTGCTGTTACCTCCCTTTCT
Vegf-a	F AGGGCAGAATCATCACGAAGT
	R AGGGTCTCGATTGGATGGCA
Tgfbi	F ACCATGGACCGGATGTTGAC
	R GGCCACCAGCATGCTAAAAC
Rspo2	F AGACGCAATAAGCGAGGTGG
	R CTGCATCGTGCACATCTGTT
β-actin	F GCTCGTCGTCGACAACGGCTC
	R CAAACATGATCTGGGTCATCTTCTC

Col-1, collagen-1; *Mmp-13*, matrix metallopeptidase-13; *Adamts4*, a disintegrin and metalloproteinase with a thrombospondin type 1 motif member 4; *Timp-1*, tissue inhibitor of metalloproteinases-1; *Sox6*, SRY-Box transcription 6; *Runx2*, runt-related transcription factor 2; *Ki67*, antigen Ki67; *Gdf5*, growth/differentiation factor 5; *Vegf-a*, vascular endothelial growth factor A; *Tgfbi*, transforming growth factor-beta-induced gene; *Rspo2*, R-spondin 2; F, forward; R, reverse.

tions of 21 ℃ and a 12-h light-dark cycle. Following a one-week acclimatization period, subsequent experiments were performed. All animal-related experiments in this study were approved by the animal ethics committee of Wendeng Hospital of Traditional Chinese Orthopedics and Traumatology of Shandong Province (approval no. LL20240201).

In Vitro Culture and Treatments of Mouse Menisci

A total of 10 mice were randomly selected for the collection of *en bloc* meniscal samples, which were then cultured in dishes containing Dulbecco's Modified Eagle Medium (DMEM; iCell-0001, iCell Bioscience Inc., Shanghai, China) containing 10% fetal bovine serum (FBS; iCell-0500, iCell Bioscience Inc., Shanghai, China). Following normal culture for 24 h, five meniscal samples were kept under normal culture conditions for three days as the negative control group (NC), while the remaining five samples were treated with the additional UB (50 μM) for three days as the experimental group (UB). Afterward, samples were washed with phosphate-buffered saline (PBS; C0221A, Beyotime, Shanghai, China) and used for subsequent experiments.

Establishment and Treatment of MIOA Mouse Models

The establishment of meniscus injury-induced osteoarthritis (MIOA) was performed based on the protocol described in a previous study [15]. Briefly, the remaining 20 mice were divided into four groups: Sham, MIOA, MIOA+Vehicle, and MIOA+UB, with five mice in each group. Mice were initially anesthetized using pentobarbital sodium (60 mg/kg; P3761, Sigma-Aldrich, Saint Louis, MO, USA) via intraperitoneal injection. In the Sham group, the joint cavity was exposed and immediately closed. For MIOA group, mice received surgery for causing meniscus injury and inducing osteoarthritis (OA); Mice in the MIOA+UB group received subcutaneous UB injection (50 mg/kg) dissolved in a vehicle solution (1% DMSO dissolved in normal saline; DMSO: ST038, Beyotime, Shanghai, China; normal saline: ST341, Beyotime, Shanghai, China) for 14 consecutive days [16]. Conversely, mice in the MIOA+Vehicle group received subcutaneous injection of the vehicle alone in equal volume for the same duration. The mice were euthanized using pentobarbital sodium (180 mg/kg; P3761, Sigma-Aldrich, Saint Louis, MO, USA) through intraperitoneal injection, and knee joint samples were collected 12 weeks after the surgery. All tissue samples were immediately frozen in liquid nitrogen and stored at –80 ℃ for subsequent experiments.

Hematoxylin-Eosin (H&E) Staining

A portion of each collected tissue was taken from –80 ℃ storage and placed in 4% paraformaldehyde (P0099, Beyotime, Shanghai, China) overnight. Following fixation, the tissues were embedded in paraffin and sliced into 7-μm-thick sections. Afterward, sections were dewaxed, hydrated, and stained using a hematoxylin-eosin staining assay kit (C0105S, Beyotime, Shanghai, China). Finally, observation was conducted through an optical microscope (CX31, Olympus, Tokyo, Japan).

5-Bromo-2′-Deoxyuridine (BrdU) Staining

According to the manufacturer's instruction, slides containing meniscal cells were well-prepared and stained with 5-Bromo-2′-deoxyuridine (BrdU) (ST1056, Beyotime, Shanghai, China) for 4 h. Subsequently, tissue samples were observed under a microscope (CKX53, OLYMPUS, Tokyo, Japan) and staining results were quantified by ImageJ software (version 1.48, National Institutes of Health, Rockville, MD, USA).

Western Blot

Tissue samples were minced into small pieces and homogenized by ultrasound in RIPA buffer (P0013E, Beyotime, Shanghai, China) containing 1 mmol/L PMSF (ST505, Beyotime, Shanghai, China). Total proteins were obtained from the supernatant. Proteins were separated by sodium dodecyl sulfate-polyacrylamide gel electrophoresis (SDS-PAGE; P0012A, Beyotime, Shanghai, China) and transferred to a polyvinylidene difluoride (PVDF) membrane (IPVH00010, Millipore, Billerica, MA, USA). Membranes were blocked with 5% skim milk for one hour and then incubated with the primary antibody at 4 ℃ overnight. Primary antibodies included anti-proliferating cell nuclear antigen (PCNA; 1:1000 dilution; ab92552, Abcam, Cambridge, MA, USA), anti-matrix metallopeptidase-13 (MMP-13; 1:10,000 dilution; ab39012, Abcam, Cambridge, MA, USA), anti-vascular endothelial growth factor (VEGF; 1:1000 dilution; MA5-13182, Invitrogen, Carlsbad, CA, USA), anti-collagen-1 (COL-1; 1:1000 dilution; PA1-26204, Invitrogen, Carlsbad, CA, USA), and anti-glyceraldehyde-3-phosphate dehydrogenase (GAPDH; 1:1000 dilution; ab9485, Abcam, Cambridge, MA, USA). Following membrane washing with TBST (ST673, Beyotime, Shanghai, China), they were incubated with horseradish peroxidase (HRP)-conjugated secondary antibody (1:2000 dilution; ab7090, Abcam, Cambridge, MA, USA) for 1 h at room temperature. Reactive bands were visualized using enhanced chemiluminescence (ECL; P0018S, Beyotime, Shanghai, China), and grey values were analyzed using ImageJ software (version 1.48, National Institutes of Health, Rockville, MD, USA).

Statistical Analysis

All data were analyzed by the GraphPad Prism 8.0.2 (GraphPad Software, La Jolla, CA, USA) and presented as the mean ± standard deviation (SD) of five independent experiments. Statistical analysis was performed using analysis of variance (ANOVA) followed by Tukey's post hoc test. A value of $p < 0.05$ was considered statistically significant.

Results

Immunofluorescence

The cell morphology was observed with a high-power microscope, as shown in Fig. 1. The cells have a fusiform structure. Mice meniscus cell surface markers COL-1 and COL-2 were stained by immunofluorescence. Fig. 1B,C showed that both COL-1 and COL-2 had strong positive signals.

UB Ameliorated Inflammation in Meniscal Cells

Initially, we conducted a cytotoxicity assay to evaluate the effects of UB treatment on meniscal cells. As shown in Fig. 2A, after treating meniscal cells with UB for two days (left) or five days (right), cell viability remained unchanged until the UB concentration reached 120 µM ($p < 0.001$) and 140 µM ($p < 0.001$), demonstrating that UB did not affect cell viability when the concentration of UB did not exceed 100 µM. Moreover, the cytotoxicity assay involving UB cotreatment with IL-1β (1 ng/mL) is illustrated in Fig. 2B. Notably, even when used in conjunction with IL-1β for two days or five days, UB concentrations of up to 100 µM did not affect the viability of meniscal cells. In Fig. 2C, the TNF-α levels in cell culture supernatant are depicted, demonstrating that the 12-h administration of UB decreased the level of proinflammatory cytokine TNF-α at concentrations of 30 µM ($p < 0.001$), 50 µM ($p < 0.001$), and 100 µM ($p < 0.001$) compared to normally cultured meniscal cells. Moreover, the 12-h administration of IL-1β significantly increased the basal TNF-α levels in meniscal cells ($p < 0.001$), which were subsequently decreased by UB administration at concentrations of 30 µM ($p < 0.001$), 50 µM ($p < 0.001$), and 100 µM ($p < 0.001$). These results show the anti-inflammatory effect of UB in meniscal cells. Given that the concentration of 100 µM represented the upper limit of safe UB dosage and the inhibitory effect of UB at 50 µM on TNF-α was prominent, UB at 50 µM was used for subsequent experiments. Fig. 2D illustrates the suppressive effect of 50-µM UB on the IL-1β levels ($p < 0.001$) in cell culture supernatant after treating meniscal cells for 12 h, further proving the anti-inflammatory effect of UB.

UB Promoted mRNA Expression of Extracellular Matrix (ECM) Proteins while Inhibiting the mRNA Expression of ECM-Degrading Enzymes in Meniscal Cells

As shown in Fig. 3, following treatment with 50-µM UB for 12 h, meniscal cells exhibited significantly increased mRNA levels of extracellular matrix proteins, including *Col-1* ($p < 0.001$), *Col-2* ($p < 0.001$), *Col-3* ($p < 0.001$), tissue inhibitor of metalloproteinases-1 (*Timp-1*) ($p < 0.001$), and Aggrecan ($p < 0.001$). Conversely, cells treated with 50-µM UB for 12 h displayed significantly lower mRNA levels of *Mmp-13* ($p < 0.001$), a disintegrin and metalloproteinase with a thrombospondin type 1 motif member 4 (*Adamts4*) ($p < 0.001$), and *Adamts5* ($p < 0.001$) compared to normally cultured cells. Notably, these genes are all related to extracellular matrix (ECM) degra-

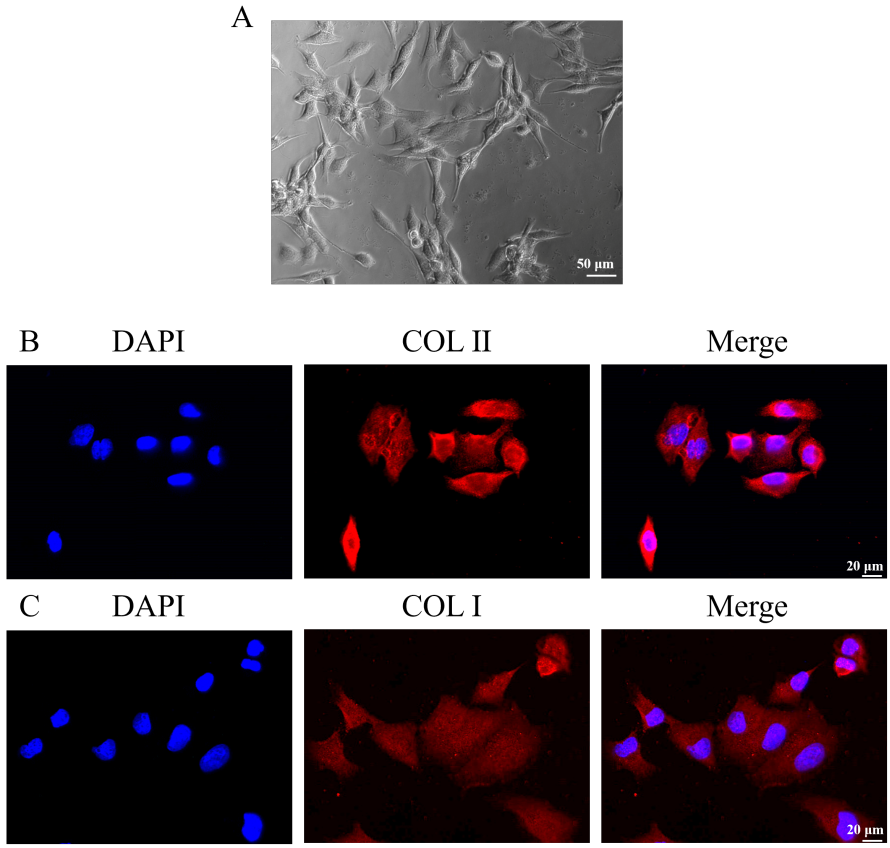

Fig. 1. Identification and surface markers of mouse meniscus cells. (A) Morphological picture of mouse meniscus cells. (B,C) Mice meniscus cells were stained by COL-1 and COL-2 immunofluorescence.

dation [17]. These results demonstrate the effect of UB in promoting ECM development and progression in meniscal cells.

UB Promoted the mRNA Expression of Joint Formation-Related Genes in Meniscal Cells

Fig. 4 demonstrates that UB increased the mRNA levels of SRY-Box Transcription Factor 6 (*Sox6*) ($p < 0.001$), *Sox9* ($p < 0.001$), antigen Ki67 (*Ki67*) ($p < 0.001$), growth/differentiation factor 5 (*Gdf5*) ($p < 0.001$), vascular endothelial growth factor A (*Vegf-a*) ($p < 0.001$), transforming growth factor-beta-induced gene (*Tgfbi*) ($p < 0.001$), and R-spondin 2 (*Rspo2*) ($p < 0.001$), while decreasing the mRNA level of runt-related transcription factor 2 (*Runx2*) ($p < 0.001$) in meniscal cells. These results demonstrate the promotional effects of UB on meniscal cell progression and thus, potentially on joint formation.

UB Promoted Meniscal Cell Proliferation

The results depicted in Fig. 5A,B from BrdU staining reveal that UB-treated meniscal cells exhibited significantly increased BrdU staining compared to normally cultured meniscal cells ($p < 0.001$), indicating a promotion of cell proliferation by UB.

UB Promoted ECM Development and Cell Proliferation in Menisci in Vitro

The western blot results (Fig. 6A,B) reveal that *in vitro* treatment of menisci with UB led to increased protein levels of PCNA ($p < 0.001$), COL-1 ($p < 0.001$), and VEGF ($p < 0.001$), while the protein level of MMP-13 was decreased ($p < 0.001$). PCNA and VEGF are known to induce and participate in cell proliferation [18,19]. Additionally, COL-1 is a key ECM protein and a major component of ECM [20,21], while MMPs, especially MMP-13, are contributors to ECM degradation [22]. Therefore, these results collectively suggest that UB promotes ECM development in menisci and the progression of menisci *in vitro*.

UB Ameliorated the Severity of MIOA in Vivo

The western blot results (Fig. 7A,B) reveal that in meniscal tissues, MIOA decreased protein levels of cell proliferation-related PCNA ($p < 0.001$) and VEGF ($p < 0.001$), as well as ECM formation-related COL-1 ($p < 0.001$) while increasing the protein level of ECM degradation-related MMP-13 ($p < 0.001$). However, these alterations in protein levels observed in mouse meniscal tissues were reversed by UB administration (PCNA, $p < 0.001$; COL-1, $p < 0.001$; VEGF, $p < 0.001$; MMP-13, $p < 0.001$), indicating that UB promotes cell proliferation and

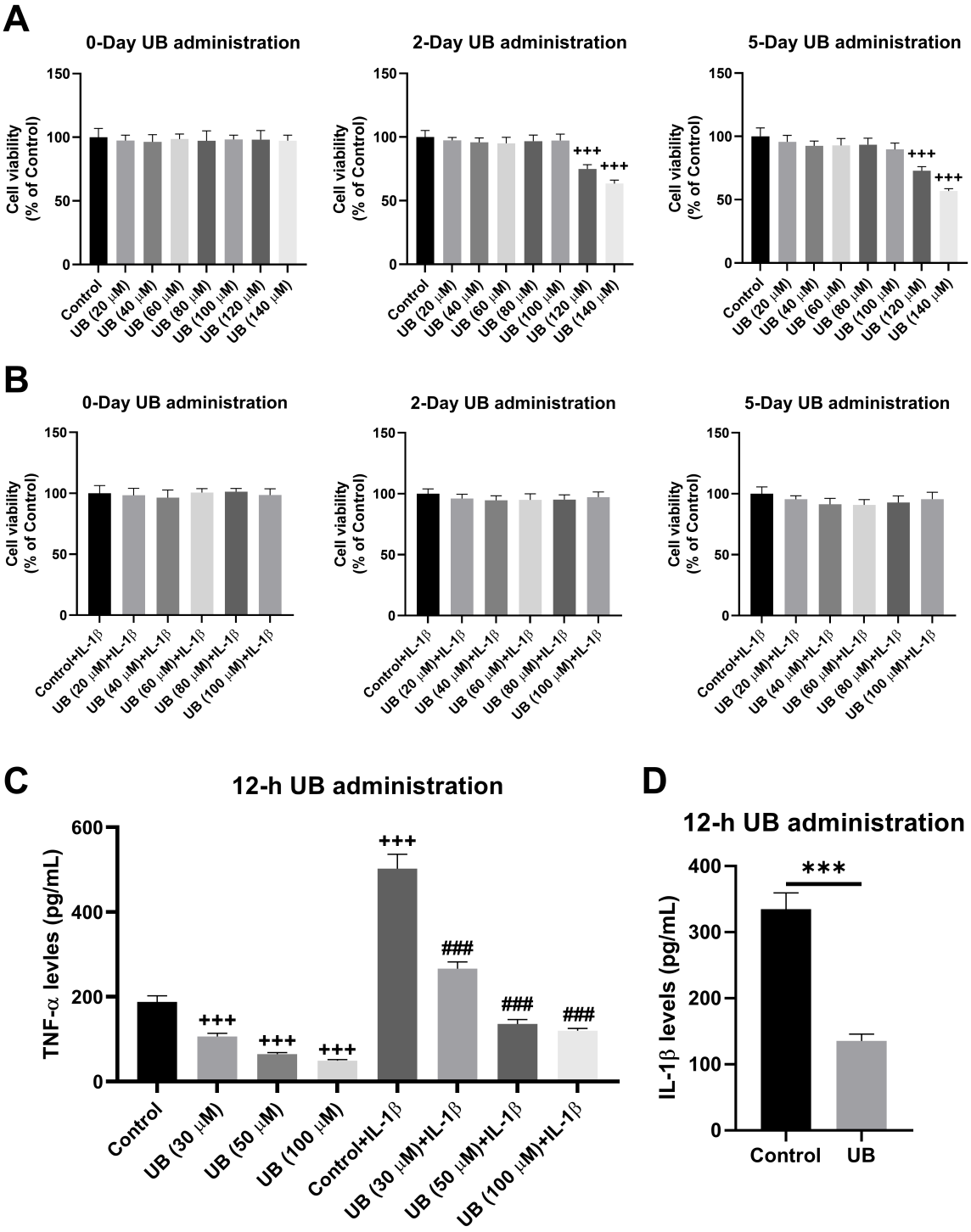

Fig. 2. Urolithin B (UB) ameliorated inflammation in meniscal cells. (A) Cell viability of meniscal cells treated with UB at different concentrations for 0 days, 2 days, or 5 days. (B) Cell viability of meniscal cells pretreated with interleukin-1beta (IL-1β) and then treated with UB at different concentrations for 0 days, 2 days, or 5 days. Protein levels of (C) tumor necrosis factor-alpha (TNF-α) and (D) IL-1β in the culture supernatant of differently treated meniscal cells. N = 5. Control, normally cultured meniscal cells; UB (20 μM), normal meniscal cells treated with 20-μM of UB; Control+IL-1β, normal meniscal cells treated with 12-h of IL-1β (1 ng/mL) and then normally cultured; UB (20 μM)+IL-1β, meniscal cells treated with 12-h IL-1β and then treated with 20-μM of UB; UB, meniscal cells treated with 50-μM of UB. +++$p < 0.001$ vs. Control; ###$p < 0.001$ vs. Control+IL-1β; ***$p < 0.001$.

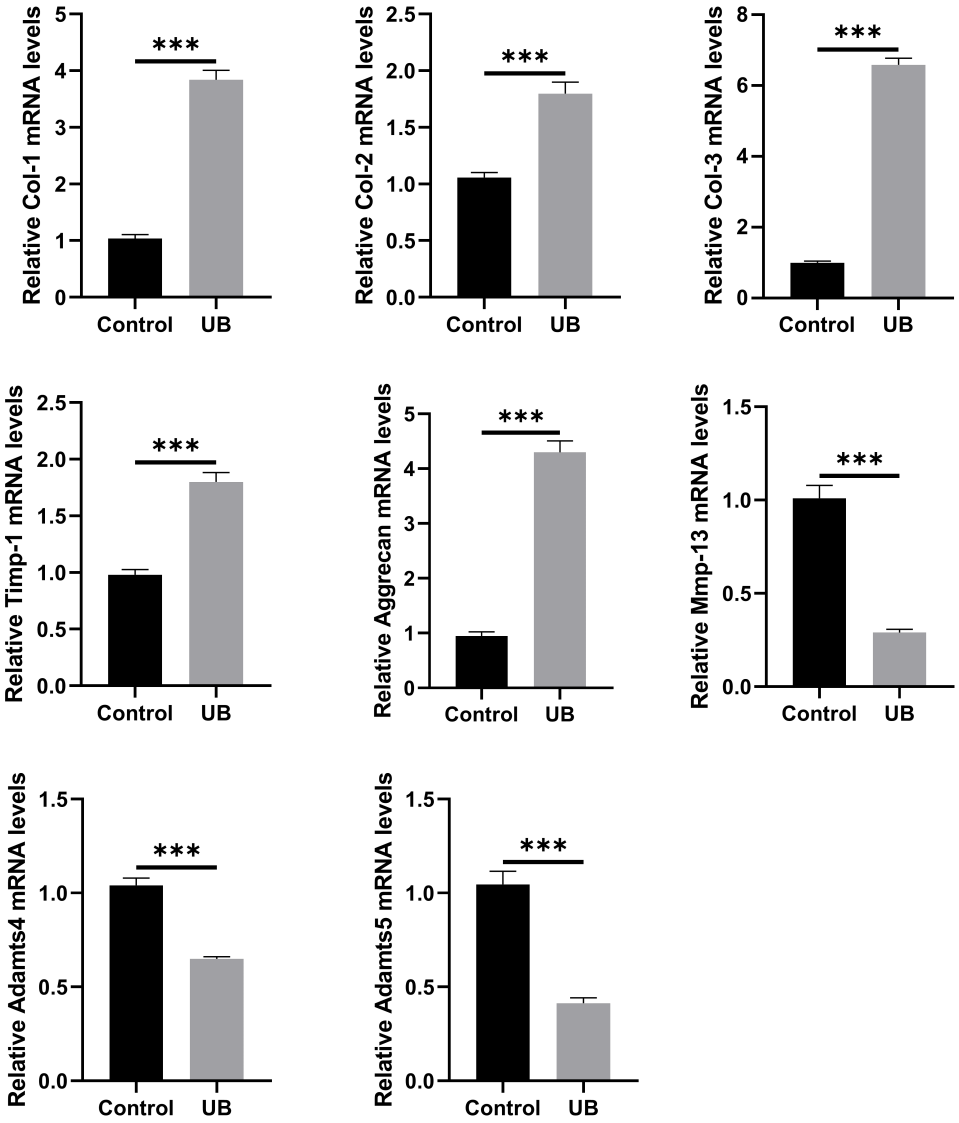

Fig. 3. UB promoted mRNA expression of extracellular matrix (ECM) proteins while inhibiting the mRNA expression of ECM protein degrading enzymes in meniscal cells. The mRNA levels *Col-1*, *Col-2*, *Col-3*, *Timp-1*, Aggrecan, *Mmp-13*, *Adamts4*, and *Adamts5* in meniscal cells. N = 5. ***$p < 0.001$.

ECM progression in MIOA. Moreover, in meniscal tissues of MIOA mice, the levels of TNF-α (Fig. 7C, $p < 0.001$), IL-1β (Fig. 7D, $p < 0.001$), IL-6 (Fig. 7E, $p < 0.001$), and IFN-γ (Fig. 7F, $p < 0.001$) were all increased compared to meniscal tissues of Sham mice. In meniscal tissues of UB-treated MIOA mice, levels of TNF-α ($p < 0.001$), IL-1β ($p < 0.001$), IL-6 ($p < 0.001$), and IFN-γ ($p < 0.001$) were decreased compared to those in meniscal tissues of Vehicle-treated MIOA mice. These results indicate that UB has anti-inflammatory effects in meniscal tissues. Furthermore, representative hematoxylin-eosin (H&E) staining results presented in Fig. 8 demonstrate that knee joints of MIOA mice exhibited cartilage erosion in the femur and tibia and a decrease of stroma resident cell number (indicated by the red boxes), whereas these changes were ameliorated by UB treatment in knee joints of MIOA+UB mice. These findings collectively suggest the efficacy of UB in promoting meniscus repair, improving OA symptoms, and ameliorating OA severity.

Discussion

Research has demonstrated that meniscus injury or dysfunction increases the risk of knee OA [7]. This study validates the efficacy of UB in facilitating meniscal repair, suggesting its potential clinical utility in preventing or ameliorating knee OA.

The meniscus primarily comprises water (72%) and collagen fibers (22%) and is mainly made of collagen-1 (COL-1) [23]. Additionally, suppressed levels of ECM pro-

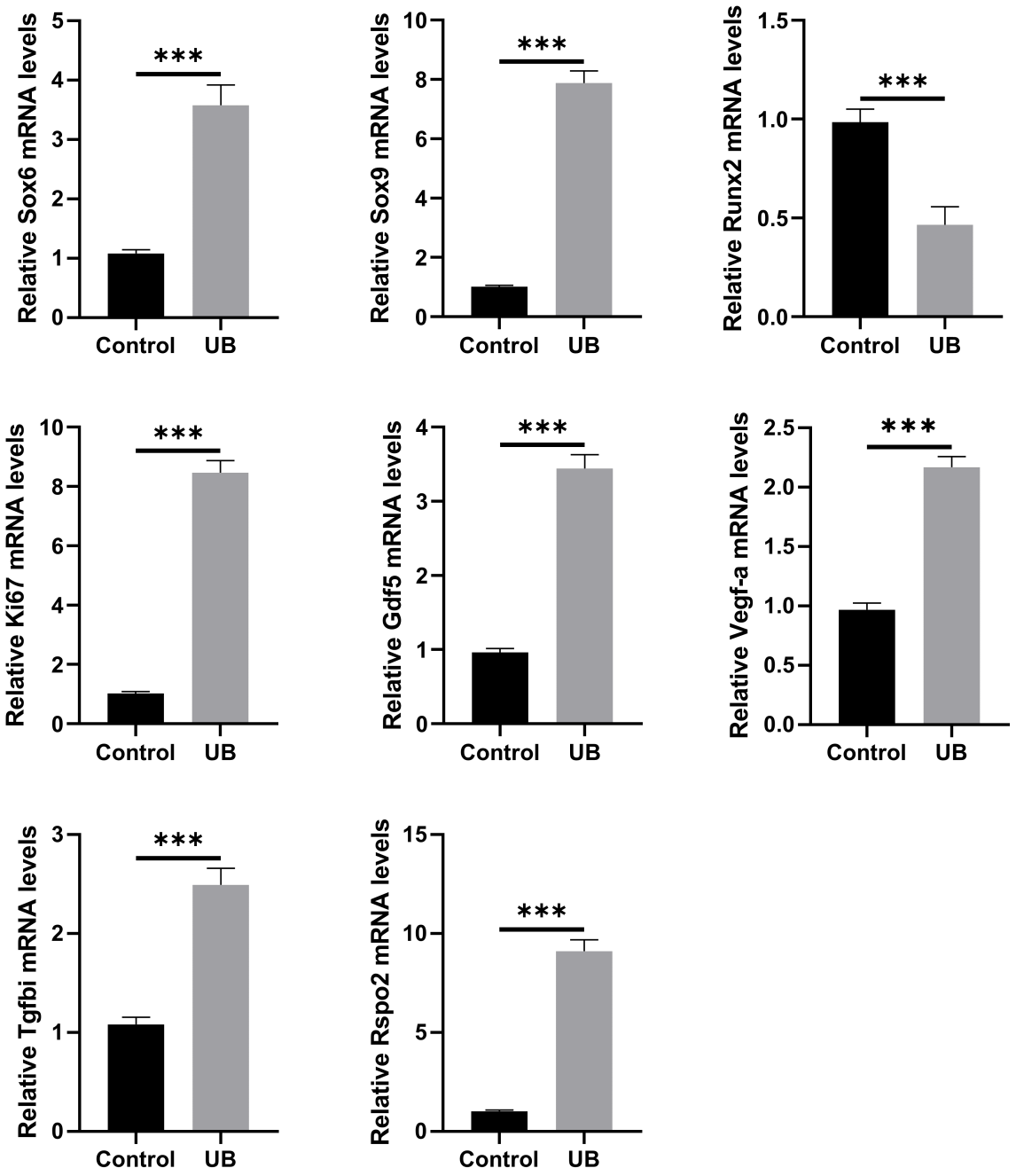

Fig. 4. UB promoted the mRNA expression of joint formation-related genes in meniscal cells. The mRNA levels of SRY-Box transcription factor 6 (*Sox6*), *Sox9*, runt-related transcription factor 2 (*Runx2*), antigen Ki67 (*Ki67*), growth/differentiation factor 5 (*Gdf5*); vascular endothelial growth factor A (*Vegf-a*), transforming growth factor-beta-induced gene (*Tgfbi*), and R-spondin 2 (*Rspo2*) in meniscal cells. N = 5. ***$p < 0.001$.

teins, including COL-2, can induce dysfunctional menisci and subsequently contribute to progressive OA [24]. Our study reveals that UB increased mRNA expression levels of *Col-1*, *Col-2*, and *Col-3*, as well as COL-1 protein levels, suggesting its effect on promoting the regeneration and progression of meniscal cells or tissues. Moreover, since meniscus vascularity is critical for meniscal repair [25], the increase in VEGF protein levels represented the enhanced meniscus regeneration and repair induced by UB. *Runx2*, which is overexpressed in cartilage samples from OA patients and animal models, has been identified as a central pathological factor in OA initiation and is associated with pathological changes in joint tissues, including the meniscus [26,27]. *Runx2* plays a critical role in OA pathogenesis and holds potential as a therapeutic target for OA [27]. Moreover, *Runx2* directly regulates catabolic enzymes such

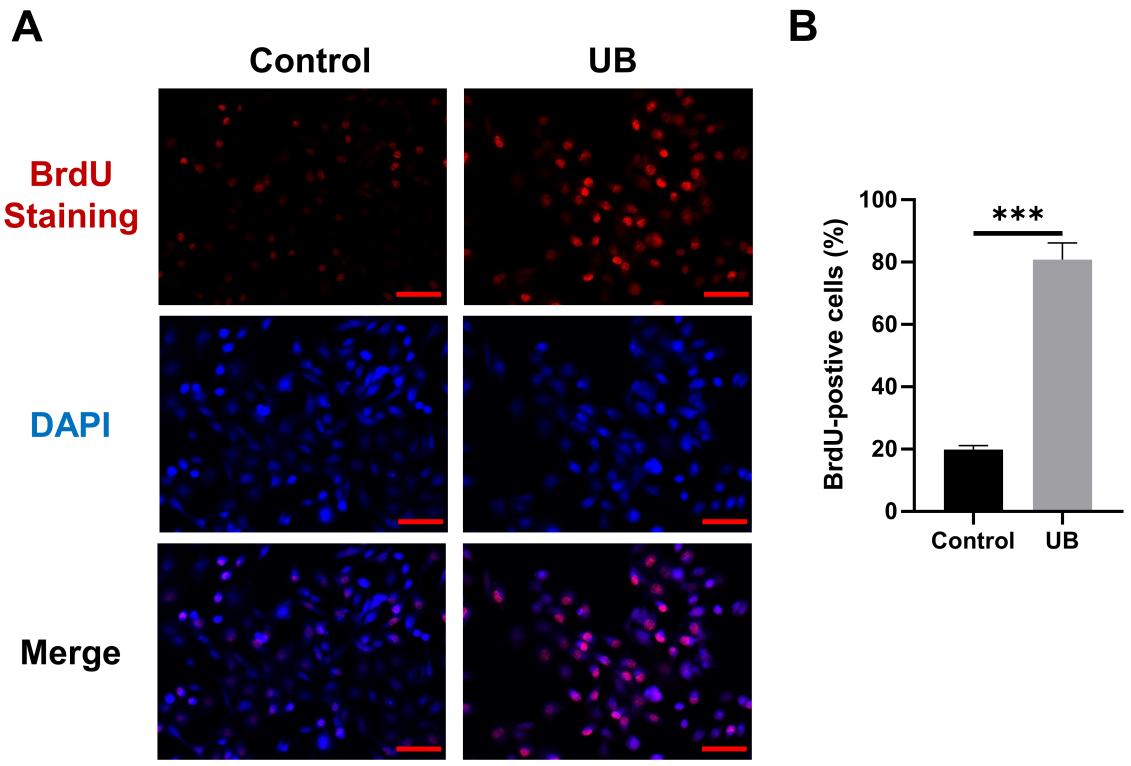

Fig. 5. UB promoted meniscal cell proliferation. (A,B) Representative images (A) and corresponding quantifications (B) of 5-Bromo-2′-deoxyuridine (BrdU) staining of meniscal cells (scale: 50 μm). N = 5. ***$p < 0.001$. DAPI, 4′,6-diamidino-2-phenylindole.

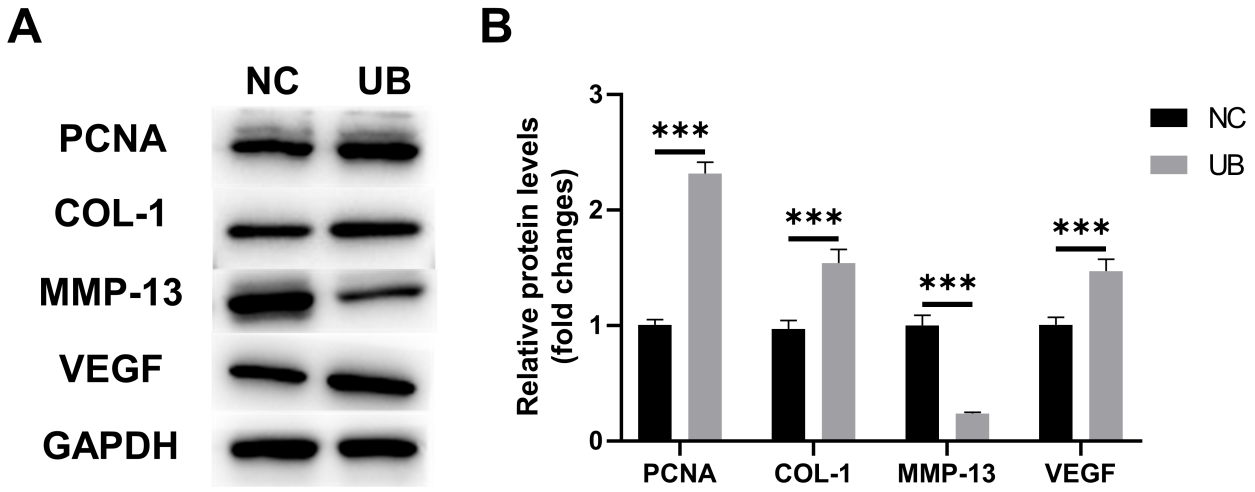

Fig. 6. UB promoted ECM development and cell proliferation in menisci *in vitro*. (A,B) Representative images of western blot (A) and quantification of proteins (B) in menisci cultured *in vitro*. N = 5. PCNA, proliferating cell nuclear antigen; MMP-13, matrix metallopeptidase-13; VEGF, vascular endothelial growth factor; COL-1, collagen-1; GAPDH, glyceraldehyde-3-phosphate dehydrogenase; NC, negative control group; UB, menisci treated with 50-μM UB for 3 days. ***$p < 0.001$.

as MMP-13 and Adamts5 [28]. Reports suggest that MMP-13 expression is increased in OA rat models [29,30]. Down-regulation of MMP-13 has been associated with inhibited articular cartilage degeneration and OA progression, while overexpression of MMP-13 in cartilage induces OA-like phenotypes in mouse models [31]. Moreover, MMP-13, the primary collagenase in OA, is significantly increased in the synovium obtained from medial meniscus transection (MMT) OA mouse models [32], consistent with the results of this study, demonstrating increased MMP-13 pro-

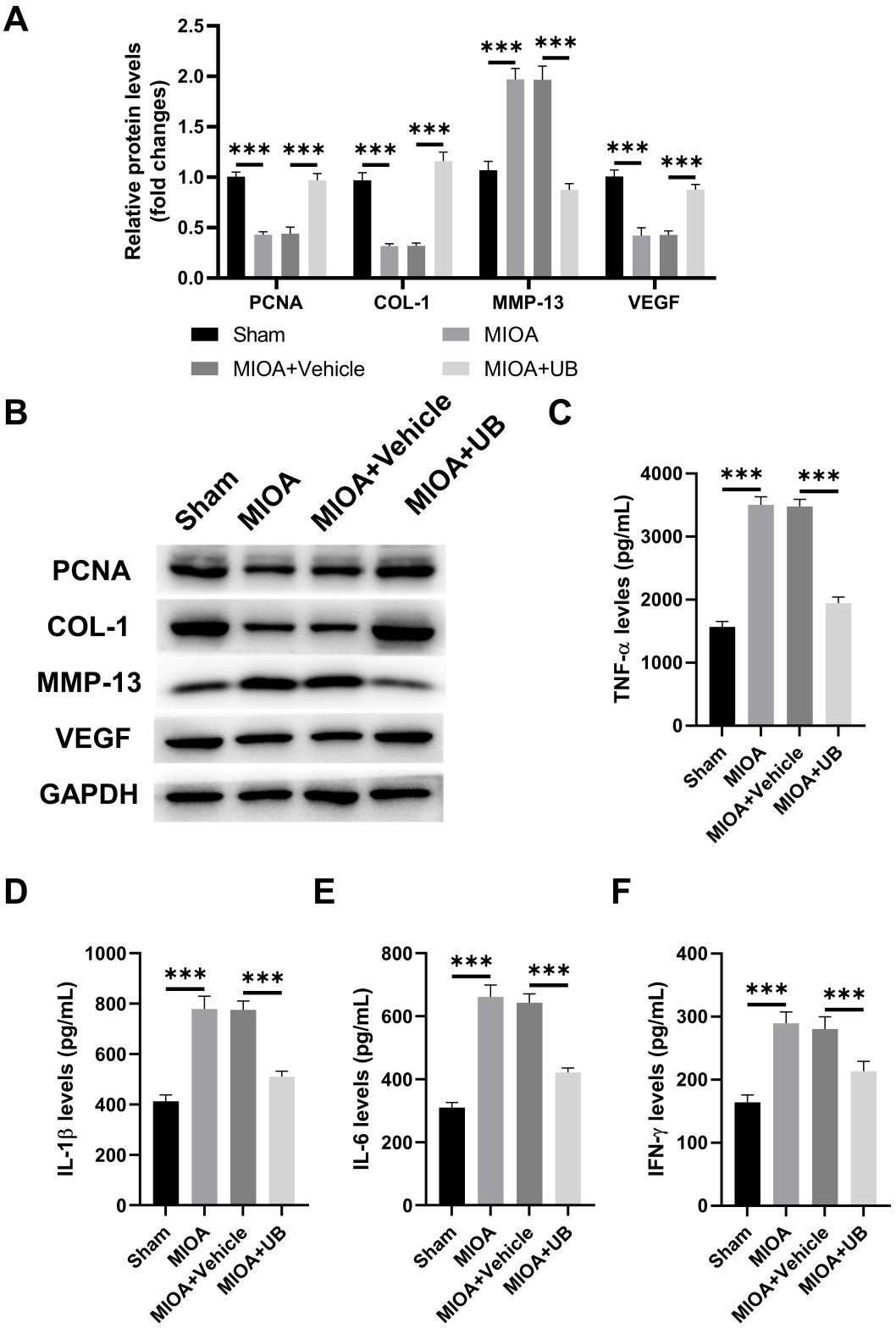

Fig. 7. UB ameliorated the severity of meniscus injury-induced osteoarthritis (MIOA) *in vivo*. The (A) quantification and (B) representative western blot images of proteins in meniscal tissues form mice models. The protein levels of (C) TNF-α, (D) IL-1β, (E) IL-6, and (F) interferon-gamma (IFN-γ) in meniscal tissues from mice models. N = 5. Sham, mice received sham surgery; MIOA, mice received surgery for causing meniscus injury and inducing osteoarthritis (OA); MIOA+Vehicle, MIOA mice treated with Vehicle (1% DMSO dissolved in 0.9% normal saline); MIOA+UB, MIOA mice treated with UB (50 mg/kg dissolved in Vehicle). ***$p < 0.001$.

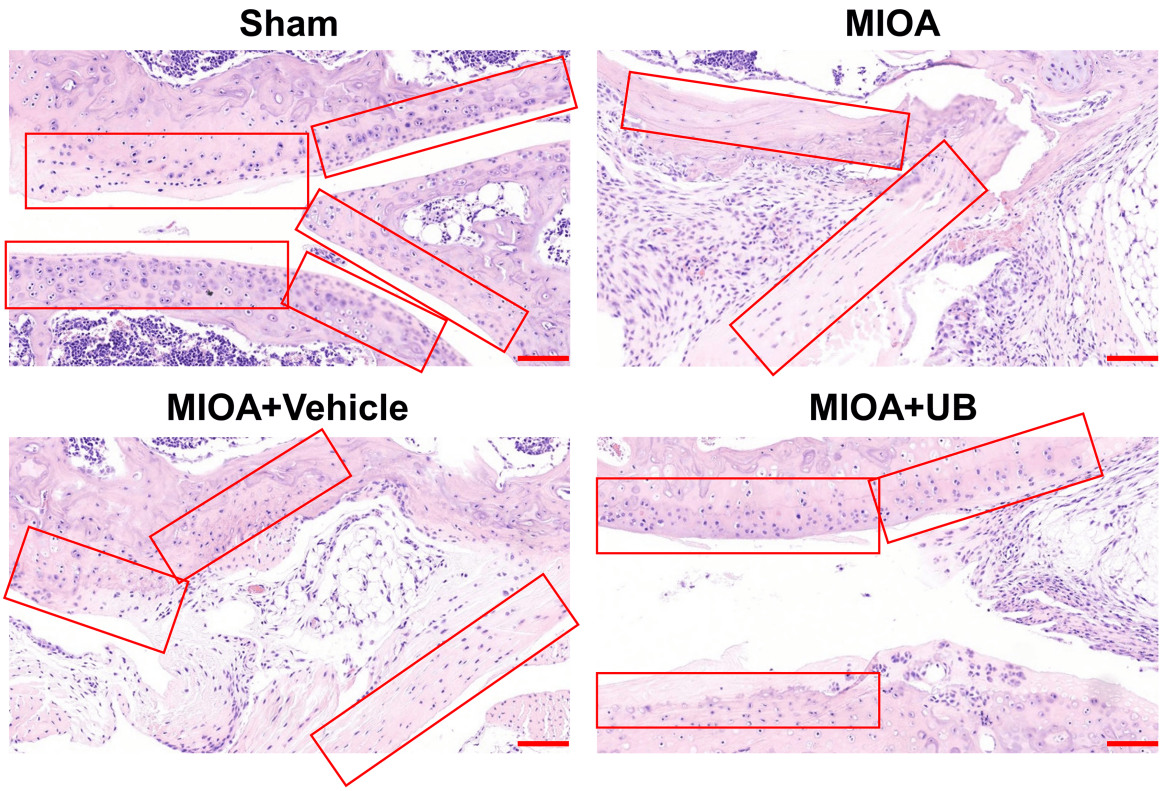

Fig. 8. UB ameliorated the severity of MIOA *in vivo*. The representative hematoxylin-eosin (H&E) staining results of knee joints obtained from mice (scale bar: 200 μm; red boxes indicated the stroma resident cells).

tein levels in meniscal tissues of MIOA mice. Furthermore, *Adamts* are essential proteases in OA cartilage tissues from humans and animals, playing critical roles in the degradation of Aggrecan, a major component of the ECM. Studies have shown that Adamts5 deletion protects joints from cartilage destruction and prevents OA exacerbation [33,34]. In this study, UB suppressed Runx2, MMP-13, and Adamts, while promoting Aggrecan, demonstrating its ability to mitigate OA progression.

Post-traumatic OA manifests in joints following injury and constitutes a subtype of OA. Knee injury has been established as a significant risk factor for knee OA, increasing the likelihood of OA development in the knee joint fivefold [35]. In this study, we induced knee OA in mice by causing meniscus injury. At 12 weeks post-surgery, the meniscal tissues of these mice exhibited symptoms indicative of ECM degradation and inflammation. Pain is a primary clinical symptom of OA and serves as a clinical indicator of tissue damage, inflammation, or nervous system disorders [36–38]. In this study, we demonstrated that UB could reduce inflammation in both meniscal cells and tissues, proving its potential effect on ameliorating OA symptoms and progression. Moreover, it has been reported that cytokines, including TNF-α, play critical roles in triggering joint inflammation. Inflammation in the joint contributes to destructive changes in the ECM, such as ECM breakdown and cartilage degradation, thus promoting OA [1]. These findings align with those observed in this study, in which increased TNF-α levels were accompanied by increased levels of ECM-degrading enzymes and decreased levels of ECM-related proteins in MIOA mouse models. In this study, administration of UB to MIOA mice was found to decrease the levels of TNF-α and ECM-degrading enzymes, while reversing the levels of ECM-related proteins. These findings support the role of UB in alleviating joint inflammation and facilitating ECM recovery during OA.

Conclusion

In summary, UB promotes meniscal repair and regeneration, potentially preventing OA pathogenesis and ameliorating OA progression. This study indicates UB as a potential therapeutic strategy for OA treatment.

Availability of Data and Materials

Data to support the findings of this study are available on reasonable request from the corresponding author.

Author Contributions

WW, HW and BC performed the research. BC and LW provided help and advice on the experiments. LW, YZ and HL contributed to the analysis and interpretation of the data. All authors were involved in the drafting and critical

revision of the manuscript. All authors read and approved the final manuscript. All authors have participated sufficiently in the work to take public responsibility for appropriate portions of the content and agreed to be accountable for all aspects of the work in ensuring that questions related to its accuracy or integrity.

Ethics Approval and Consent to Participate

All animal-related experiments in this study were approved by the animal ethics committee of Wendeng Hospital of Traditional Chinese Orthopedics and Traumatology of Shandong Province (approval no. LL20240201).

Acknowledgment

Not applicable.

Funding

This research received no external funding.

Conflict of Interest

The authors declare no conflict of interest.

References

[1] Yao Q, Wu X, Tao C, Gong W, Chen M, Qu M, *et al*. Osteoarthritis: pathogenic signaling pathways and therapeutic targets. Signal Transduction and Targeted Therapy. 2023; 8: 56.

[2] Jang S, Lee K, Ju JH. Recent Updates of Diagnosis, Pathophysiology, and Treatment on Osteoarthritis of the Knee. International Journal of Molecular Sciences. 2021; 22: 2619.

[3] Hall M, van der Esch M, Hinman RS, Peat G, de Zwart A, Quicke JG, *et al*. How does hip osteoarthritis differ from knee osteoarthritis? Osteoarthritis and Cartilage. 2022; 30: 32–41.

[4] Kolasinski SL, Neogi T, Hochberg MC, Oatis C, Guyatt G, Block J, *et al*. 2019 American College of Rheumatology/Arthritis Foundation Guideline for the Management of Osteoarthritis of the Hand, Hip, and Knee. Arthritis & Rheumatology (Hoboken, N.J.). 2020; 72: 220–233.

[5] Abramoff B, Caldera FE. Osteoarthritis: Pathology, Diagnosis, and Treatment Options. The Medical Clinics of North America. 2020; 104: 293–311.

[6] Ozeki N, Koga H, Sekiya I. Degenerative Meniscus in Knee Osteoarthritis: From Pathology to Treatment. Life (Basel). 2022; 12: 603.

[7] Ozeki N, Seil R, Krych AJ, Koga H. Surgical treatment of complex meniscus tear and disease: state of the art. Journal of ISAKOS: Joint Disorders & Orthopaedic Sports Medicine. 2021; 6: 35–45.

[8] Twomey-Kozak J, Jayasuriya CT. Meniscus Repair and Regeneration: A Systematic Review from a Basic and Translational Science Perspective. Clinics in Sports Medicine. 2020; 39: 125–163.

[9] Iglesias-Aguirre CE, Cortés-Martín A, Ávila-Gálvez MÁ, Giménez-Bastida JA, Selma MV, González-Sarrías A, *et al*. Main drivers of (poly)phenol effects on human health: metabolite production and/or gut microbiota-associated metabotypes? Food & Function. 2021; 12: 10324–10355.

[10] Cortés-Martín A, Selma MV, Tomás-Barberán FA, González-Sarrías A, Espín JC. Where to Look into the Puzzle of Polyphenols and Health? The Postbiotics and Gut Microbiota Associated with Human Metabotypes. Molecular Nutrition & Food Research. 2020; 64: e1900952.

[11] Al-Harbi SA, Abdulrahman AO, Zamzami MA, Khan MI. Urolithins: The Gut Based Polyphenol Metabolites of Ellagitannins in Cancer Prevention, a Review. Frontiers in Nutrition. 2021; 8: 647582.

[12] García-Villalba R, Giménez-Bastida JA, Cortés-Martín A, Ávila-Gálvez MÁ, Tomás-Barberán FA, Selma MV, *et al*. Urolithins: a Comprehensive Update on their Metabolism, Bioactivity, and Associated Gut Microbiota. Molecular Nutrition & Food Research. 2022; 66: e2101019.

[13] Chen P, Guo Z, Chen F, Wu Y, Zhou B. Recent Advances and Perspectives on the Health Benefits of Urolithin B, A Bioactive Natural Product Derived from Ellagitannins. Frontiers in Pharmacology. 2022; 13: 917266.

[14] D'Amico D, Olmer M, Fouassier AM, Valdés P, Andreux PA, Rinsch C, *et al*. Urolithin A improves mitochondrial health, reduces cartilage degeneration, and alleviates pain in osteoarthritis. Aging Cell. 2022; 21: e13662.

[15] Fu XN, Li HW, Du N, Liang X, He SH, Guo KJ, *et al*. Erythropoietin enhances meniscal regeneration and prevents osteoarthritis formation in mice. American Journal of Translational Research. 2020; 12: 6464–6477.

[16] Lee G, Park JS, Lee EJ, Ahn JH, Kim HS. Anti-inflammatory and antioxidant mechanisms of urolithin B in activated microglia. Phytomedicine: International Journal of Phytotherapy and Phytopharmacology. 2019; 55: 50–57.

[17] Xiao J, Li Y, Cheng G, Xu G. Zoledronate promotes ECM degradation and apoptosis via Wnt/β-catenin. Open Medicine (Warsaw, Poland). 2022; 17: 768–780.

[18] González-Magaña A, Blanco FJ. Human PCNA Structure, Function and Interactions. Biomolecules. 2020; 10: 570.

[19] Wang X, Qu T, Sun C, Wang M. Bisdemethoxycurcumin Inhibits VEGF-Induced HUVECs Proliferation, Migration and Invasion through AMPK/mTOR Pathway-Dependent Autophagy Activation and Cell Cycle Arrest. Biological & Pharmaceutical Bulletin. 2022; 45: 1276–1282.

[20] Shi Z, Ren M, Rockey DC. Myocardin and myocardin-related transcription factor-A synergistically mediate actin cytoskeletal-dependent inhibition of liver fibrogenesis. American Journal of Physiology. Gastrointestinal and Liver Physiology. 2020; 318: G504–G517.

[21] Luchian I, Goriuc A, Sandu D, Covasa M. The Role of Matrix Metalloproteinases (MMP-8, MMP-9, MMP-13) in Periodontal and Peri-Implant Pathological Processes. International Journal of Molecular Sciences. 2022; 23: 1806.

[22] Hu Q, Ecker M. Overview of MMP-13 as a promising target for the treatment of osteoarthritis. International Journal of Molecular Sciences. 2021; 22: 1742.

[23] Gee SM, Posner M. Meniscus Anatomy and Basic Science. Sports Medicine and Arthroscopy Review. 2021; 29: e18–e23.

[24] Gamer LW, Pregizer S, Gamer J, Feigenson M, Ionescu A, Li Q, *et al*. The Role of Bmp2 in the Maturation and Maintenance of the Murine Knee Joint. Journal of Bone and Mineral Research: the Official Journal of the American Society for Bone and Mineral Research. 2018; 33: 1708–1717.

[25] Wells ME, Scanaliato JP, Dunn JC, Garcia EJ. Meniscal Injuries: Mechanism and Classification. Sports Medicine and Arthroscopy Review. 2021; 29: 154–157.

[26] Chen D, Kim DJ, Shen J, Zou Z, O'Keefe RJ. Runx2 plays a central role in Osteoarthritis development. Journal of Orthopaedic Translation. 2019; 23: 132–139.

[27] Wu X, Lai Y, Chen S, Zhou C, Tao C, Fu X, *et al*. Kindlin-2 preserves integrity of the articular cartilage to protect against osteoarthritis. Nature Aging. 2022; 2: 332–347.

[28] Liao L, Zhang S, Gu J, Takarada T, Yoneda Y, Huang J, *et al*. Deletion of Runx2 in Articular Chondrocytes Decelerates the Progression of DMM-Induced Osteoarthritis in Adult Mice. Scientific Reports. 2017; 7: 2371.

[29] Chien SY, Tsai CH, Liu SC, Huang CC, Lin TH, Yang YZ, *et al*. Noggin Inhibits IL-1β and BMP-2 Expression, and Attenuates Cartilage Degeneration and Subchondral Bone Destruction in Experimental Osteoarthritis. Cells. 2020; 9: 927.

[30] Hu Y, Li M, Chen XY, Huang CH, Cao HY, Wang GJ, *et al*. Gastrodin Ameliorates the Inflammation, Oxidative Stress, and Extracellular Matrix Degradation of IL-1β-Mediated Fibroblast-Like Synoviocytes via Suppressing the Gremlin-1/NF-κB Pathway. Discovery Medicine. 2024; 36: 1441–1452.

[31] Cong S, Meng Y, Wang L, Sun J, Shi Nu Er Xia Ti TB, Luo L. T-614 attenuates knee osteoarthritis via regulating Wnt/β-catenin signaling pathway. Journal of Orthopaedic Surgery and Research. 2021; 16: 403.

[32] Salazar-Noratto GE, De Nijs N, Stevens HY, Gibson G, Guldberg RE. Regional gene expression analysis of multiple tissues in an experimental animal model of post-traumatic osteoarthritis. Osteoarthritis and Cartilage. 2019; 27: 294–303.

[33] Santamaria S. ADAMTS-5: A difficult teenager turning 20. International Journal of Experimental Pathology. 2020; 101: 4–20.

[34] Malemud CJ. Inhibition of MMPs and ADAM/ADAMTS. Biochemical Pharmacology. 2019; 165: 33–40.

[35] Andersson JK, Hagert E, Brittberg M. Cartilage Injuries and Posttraumatic Osteoarthritis in the Wrist: A Review. Cartilage. 2021; 13: 156S–168S.

[36] Katz JN, Arant KR, Loeser RF. Diagnosis and Treatment of Hip and Knee Osteoarthritis: A Review. JAMA. 2021; 325: 568–578.

[37] Seifert O, Baerwald C. Interaction of pain and chronic inflammation. Zeitschrift für Rheumatologie. 2021; 80: 205–213.

[38] Baral P, Udit S, Chiu IM. Pain and immunity: implications for host defence. Nature Reviews. Immunology. 2019; 19: 433–447.